Journal of Molecular Structure 1137 (2017) 1–8

Contents lists available at ScienceDirect

Journal of Molecular Structure

journal homepage: http://www.elsevier.com/locate/molstruc

Synthesis, crystal and molecular-electronic structure, and kinetic investigation of two new sterically hindered isomeric forms of the dimethyl[methyl(phenylsulfonyl)amino]benzenesulfonyl chloride

L. Rublova [a], B. Zarychta [b], V. Olijnyk [b], B. Mykhalichko [c, *]

[a] Department of General Chemistry, Donetsk National Technical University, Donetsk 83001, Ukraine
[b] Faculty of Chemistry, Opole University, Opole 45-052, Poland
[c] Department of Burning Processes and General Chemistry, L'viv State University of Life Safety, L'viv 79007, Ukraine

ARTICLE INFO

Article history:
Received 15 November 2016
Received in revised form
3 February 2017
Accepted 4 February 2017

Keywords:
Sterically hindered derivatives of aromatic sulfonic acids
X-ray crystal structure determination
Kinetics of substitution reactions in aqueous solution
Quantum-chemical analysis
Ortho-effect

ABSTRACT

Two new structural isomers – 2,4-dimethyl-5-[methyl(phenylsulfonyl)amino]benzenesulfonyl chloride (**1**) and 2,4-dimethyl-3-[methyl(phenylsulfonyl)amino]benzenesulfonyl chloride (**2**) were synthesized by interaction of *N*-(2,4-dimethylphenyl)-*N*-methyl-benzenesulfonamide or *N*-(2,6-dimethylphenyl)-*N*-methylbenzenesulfonamide with chlorosulfonic acid. Both compounds have been structurally characterized by X-ray single crystal diffraction at 100 K. The crystals of **1** are triclinic: space group $P\overline{1}$, $a = 8.1542(2)$, $b = 11.0728(3)$, $c = 11.2680(3)$ Å, $\alpha = 116.557(3)$, $\beta = 95.155(2)$, $\gamma = 108.258(2)^\circ$, $V = 831.97(4)$ Å^3, $Z = 2$, $R = 0.0251$ for 2429 reflections; the crystals of **2** are monoclinic: space group $P2_1/c$, $a = 11.7428(2)$, $b = 11.3518(2)$, $c = 12.5886(2)$ Å, $\beta = 93.659(2)^\circ$, $V = 1674.66(5)$ Å^3, $Z = 4$, $R = 0.0269$ for 2622 reflections. The structure of both isomers is organized as molecular crystals. These sterically hindered organic molecules are cross-linked into framework by means of hydrogen bonds of C–H···O type (H···O distances are in range 2.27(2)–2.76(2) Å). The *ab initio* quantum-chemical calculations of an electronic structure of the isomeric molecules of **1** and **2** have been performed using the restricted Hartree-Fock method with a 6-31G* basis set. The calculated values of charge density concentrated on the electronegative atoms of the sterically hindered molecules are in good agreement with parameters of the intramolecular hydrogen bonds. The obtained data of the kinetic investigations of the substitution reactions in aqueous solution well correlate with stereo-chemical characteristics of the both molecules of the dimethyl[methyl(phenylsulfonyl)amino]-benzenesulfonyl chloride.

1. Introduction

Dimethyl[methyl(phenylsulfonyl)amino]benzenesulfonyl chloride belongs to the family of aromatic sulfonic acids derivatives, which are very attractive objects due to their wide applications, in particular, in industry [1], medicine [2], agriculture [3], high polymers production [4], as extraction agents [5], dyestuffs [6], detergents [7], or as heat-sensitive recording materials [8] *etc*. Throughout the long time, a specific attention of researchers has been paid to the synthesis and study of the reactivity of the sterically hindered derivatives of aromatic sulfonic acids, which stereospecific features are believed to play an important role in crucial change of some physical and chemical properties, *e.g.* of kinetic parameters of the solvolysis processes [9–13]. That is why high reactivity of bulky organic molecules of this family makes their structures more preferable agents in the organic synthesis. For instance, the bulky molecules of benzenesulfonyl chlorides derivatives show a biological activity and consequently they can be used as potential new broad-spectrum antibacterial drugs [14–17].

Currently, ascertainment of relationships between structure and reactivity of sterically hindered derivatives of aromatic sulfonic acids, in particular, the benzenesulfonyl chlorides, is one of the principal problems of organic chemistry. These bulky organic molecules can show hyperreactivity in solvolysis reactions. A dominant role in such processes belongs to the *ortho*-effect or, more broadly, proximity effect which nevertheless is a little-studied phenomenon. It can be explained by the lack of reliable structural data needed for an adequate interpretation of solvent molecules behavior in the conditions of nucleophilic attack on a crowded reaction center. Unfortunately, a quantitative

* Corresponding author.
E-mail address: mykhalitchko@email.ua (B. Mykhalichko).

http://dx.doi.org/10.1016/j.molstruc.2017.02.016
0022-2860/

interpretation of this effect is also absent in the literature.

Kinetic investigations of the hydrolysis of *ortho*-alkyl-substituted analogues of benzenesulfonyl chloride reveal that values of rate constants obtained experimentally and calculated on the basis of formalistic approach may significantly differ [18,19]. Though on the other hand, *ortho*-alkyl derivatives of benzenesulfonyl chlorides show increased reactivity in all cases of hydrolysis [20–23]. In such substitution reactions, the *ortho*-effect is defined not only by the nature of substituents, but also the stereochemical features of substrate initial state and transition state of a nucleophilic substitution process [24–26]. Therefore a combined experimental and theoretical study of the correlations between structure and reactivity of the sterically hindered organic molecules – *ortho*-alkyl derivatives of benzenesulfonyl chloride must be an investigation priority.

The synthesis, X-ray crystal structure determination of two sterically hindered isomers – 2,4-dimethyl-5-[methyl(-phenylsulfonyl)amino]-benzenesulfonyl chloride (**1**) and 2,4-dimethyl-3-[methyl(phenylsulfonyl)amino]-benzenesulfonyl chloride (**2**) (see Scheme 1), the quantum-chemical calculations of their molecular electronic structures as well as the kinetics of the neutral hydrolysis studied for both isomeric forms are reported in this article.

2. Experimental

2.1. Synthesis

The isomer **1** has been synthesized by three stages (Scheme 2*a*). At first the *N*-sulfonyl-substituted amide (C_6H_5–$SO_2N(H)$–$C_6H_3(CH_3)_2$) has been prepared in an aqueous solution at temperature of 70 °C. The 2,4-xylidine (0.04 mol, 4.8 g) has been placed in the flask containing benzenesulfonyl chloride (0.045 mol, 7.9 g) and vigorously stirred. The resulting HCl was neutralized by $NaHCO_3$. After reprecipitation out of alkaline solution, the *N*-phenylsulfonyl-2,4-xylidine yield has amounted to 7.4 g (72%). Then solution of the *N*-phenylsulfonyl-2,4-xylidine (0.0285 mol, 7.4 g) in 5% aqueous sodium hydroxide was prepared and methyl iodide (0.056 mol, 3.5 mL) was added at temperature of 80°C. As a result the white solid phase of C_6H_5–$SO_2N(CH_3)$–$C_6H_3(CH_3)_2$ has been crystallized out; the product yield has amounted to 5.9 g (80%).

Finally, C_6H_5–$SO_2N(CH_3)$–$C_6H_3(CH_3)_2$ (0.02 mol, 5.5 g) was mixed with chlorosulfonic acid at temperature of −5 °C. The reaction mixture was left for two days, and next 20 mL of chloroform was added. Contents of the reactor was poured out onto ice, washed out with water four times and dried by means of an anhydrous calcium chloride. The white solid phase of **1** was obtained after chloroform evaporation. The final product yield has amounted to 3.4 g (42%).

The isomer **2** has been synthesized by the same way, as **1** (see Scheme 2*b*). Both compounds were twice recrystallized out of isopropanol.

Single crystals suitable for an X-ray crystal structure analysis grew on the liquid-liquid interface of a two-phase system consisting out of dry dichloromethane and octane. First the crystals of **1** (1.5 g) or **2** (1.7 g) have been dissolved in 15 mL of dichloromethane. Next the solution was filtered and octane (20 mL) was dropwise added to the filtrate. At this stage it is important to prevent a mixing of two layers of dichloromethane and octane. The single crystals of **1** or **2** have crystallized out at once after evaporation of dichloromethane at room temperature.

2.2. X-ray crystal structure determination

Single crystals of the compounds **1** and **2** were mounted on the Xcalibur diffractometer (Mo K_α-radiation, $\lambda = 0.71073$ Å, graphite monochromator) equipped with a CCD detector. 180 ω oscillation images with an increment of 0.5 frame width and 20 s (**1**), 25 s (**2**) exposure per image were collected at 100.0(1) K using 60 mm crystal-to-detector distance. After integration the data set was corrected for Lorentz and polarization effects [27]. Cell parameters were obtained by a least-squares refinement based on reflection angles in the range $6.5 < 2\theta < 59.1°$. Structures were solved by direct methods applying SHELX software package [28]. All atoms were located from difference Fourier synthesis and refined by least-squares method in the full-matrix anisotropic (non-hydrogen atoms) and isotropic (hydrogen atoms) approximation. Finally, $U_{iso}(H)$ values were in the range of 1.5–2.5U_{eq}(C). The crystallographic data for the compounds **1** and **2** as well as details of X-ray experiment are listed in Table 1. The bond lengths and bond angles for both compounds are given in Tables S1 and S2, Supp. Info, respectively. Structures image was prepared by using the DIAMOND program [29]. The molecular structures and crystal packings of both isomers are presented on Fig. 1 and Fig. 2, respectively.

2.3. Kinetic measurements

Kinetic experiments have been performed under conditions of a pseudo-first order with respect to the nucleophilic reactant in 70% aqueous dioxane at temperature range 303–323 K on a Helios Gamma ultraviolet–visible spectrophotometer (298 nm for **1** and 305 nm for **2**). Thermodynamic parameters of a transition state, E_a and lg*A*, have been determined out of the Arrhenius equation by means of graphical method. The following correlations were used for calculating $\Delta H^{\neq}$ and $\Delta S^{\neq}$ [30]:

$$\Delta H^{\neq} = E_a - RT;$$

$$\Delta S^{\neq} = 2{,}303R(\lg A - \lg T - 10{,}75).$$

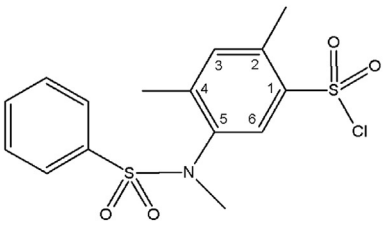

1 **2**

Scheme 1. Graphical formulas of 2,4-dimethyl-5-[methyl(phenylsulfonyl)amino]-benzenesulfonyl chloride (**1**) and 2,4-dimethyl-3-[methyl(phenylsulfonyl)amino]-benzenesulfonyl chloride (**2**).

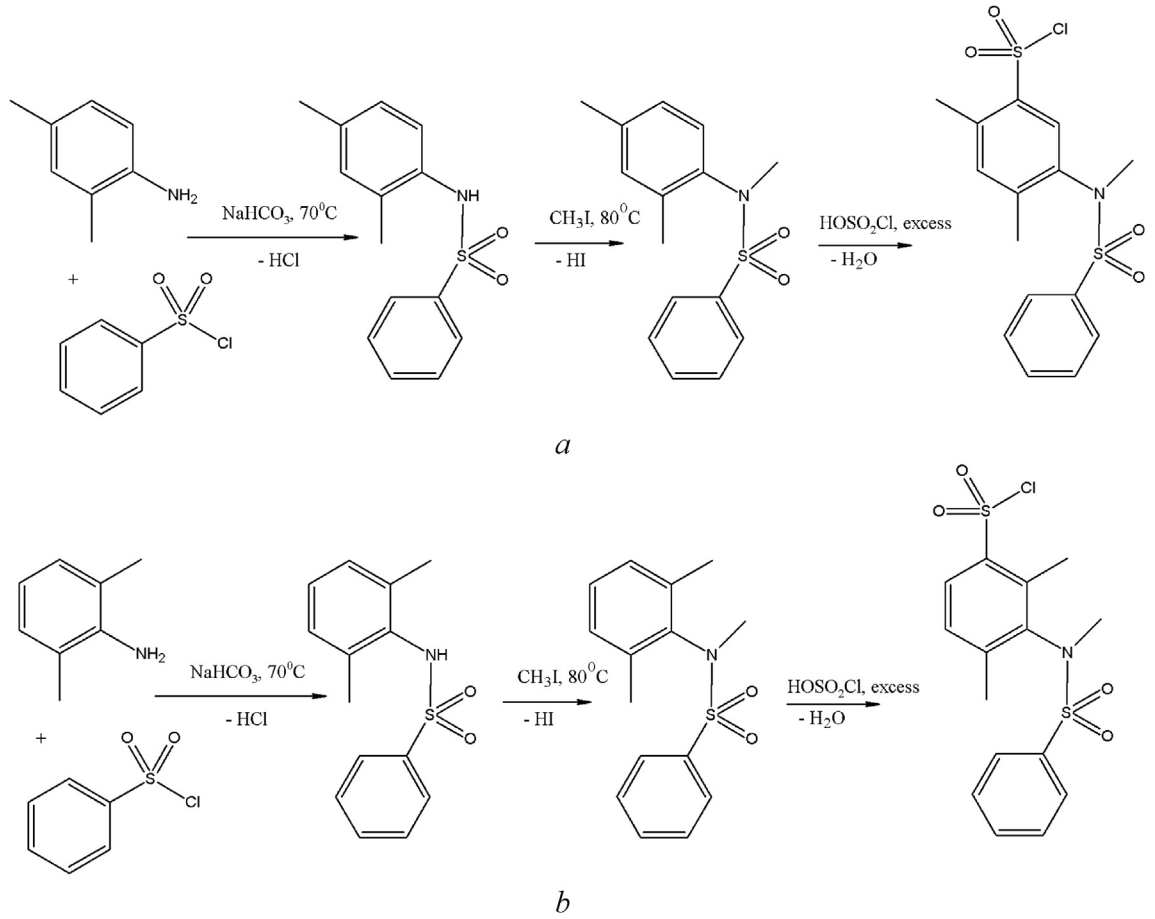

Scheme 2. Synthesis stages of **1** (*a*) and **2** (*b*).

2.4. Quantum-chemical analysis

Computer simulation of the electronic structure of two molecular isomers (**1** and **2)** has been carried out. The *ab initio* quantum-mechanical calculations (the restricted Hartree-Fock (RHF) method with a 6−31G* basis set) were performed using the HyperChem program version 8.0.6 [31]. The structures of two isomers determined by X-ray crystallography were used as starting points for

Table 1
Crystal data and experimental details for the single crystal samples of **1** and **2**.

Compound	1	2
Empirical formula	$C_{15}H_{16}S_2O_4NCl$	$C_{15}H_{16}S_2O_4NCl$
Formula weight	418.5	418.5
Color, shape	colorless, prism	colorless, plate
Crystal size [mm^3]	0.70 × 0.30 × 0.30	0.50 × 0.40 × 0.15
Space group	$P\bar{1}$	$P\,2_1/c$
a [Å]	8.1542(2)	11.7428(2)
b [Å]	11.0728(3)	11.3518(2)
c [Å]	11.2680(3)	12.5886(2)
α [°]	116.557(3)	
β [°]	95.155(2)	93.659(2)
γ [°]	108.258(2)	
V [Å^3]	831.97(4)	1674.66(5)
Z, d_c [g cm^{-3}]	2, 1.492	4, 1.483
$F(000)$	388	776
$2\theta_{max}$ [°]	49.99	49.99
Refl. collected/unique	5296/2906	10089/2934
Data/restraints/parameters	2906/0/272	2934/0/272
R_{int}, R_σ	0.0131, 0.0247	0.0138, 0.0126
Final R indices [$I > 2\sigma(I)$]	$R_1 = 0.0251$, $wR_2 = 0.0673$	$R_1 = 0.0269$, $wR_2 = 0.0725$
R indices (all data)	$R_1 = 0.0319$	$R_1 = 0.0304$
Weighing scheme	$w = [\sigma^2(F_o^2)+(0.0441P)^2 +0.00P]^{-1}$ where $P = (F_o^2+2F_c^2)/3$	$w = [\sigma^2(F_o^2)+(0.0414P)^2 +1.07P]^{-1}$ where $P = (F_o^2+2F_c^2)/3$
Goodness of fit on F^2	1.042	1.047
Largest diff. peak and hole [e Å^{-3}]	0.33(5) and −0.40(5)	0.38(5) and −0.35(5)

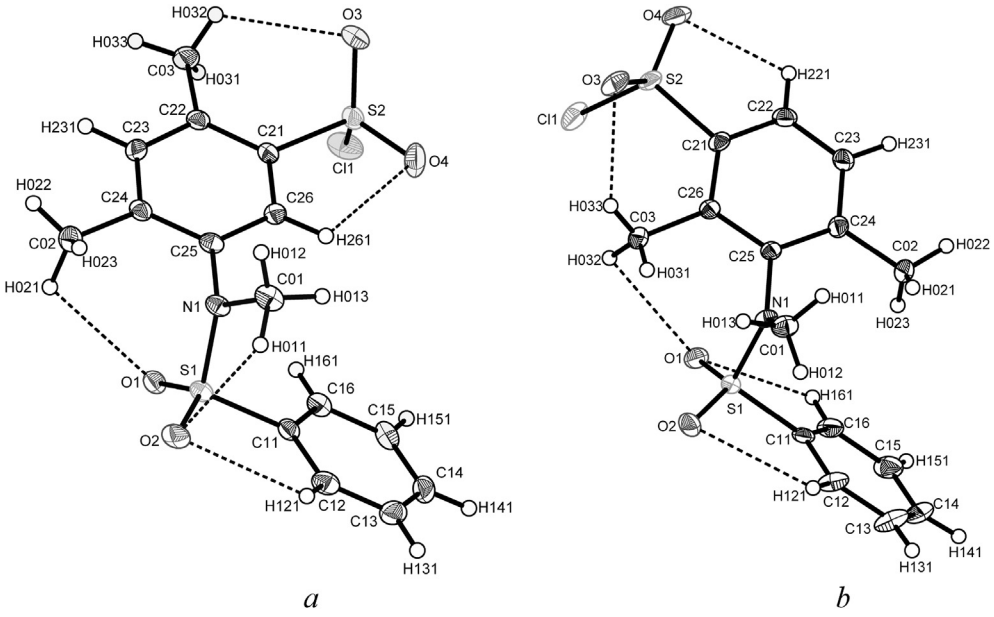

Fig. 1. The numbered atoms of two isomers: (*a*) for **1** and (*b*) for **2**. Thermal ellipsoids with 50% probability are indicated for non-hydrogen atoms.

designing molecules models. Calculations of charge density on atoms were carried out without optimization of molecules. Molecular-electronic simulations have been carried out under the hypothesis that the isomeric molecules are in the vacuum as isolated particles. Charges density distribution on atoms of isomers is represented in Fig. S1, Supp. Info. The calculated total energy and binding energy for **1** or **2** molecules in vacuum were −577535 and −41400 kJ/mol or −577121 and −40986 kJ/mol, respectively.

3. Results and discussion

3.1. Crystal structures description

Data obtained from X-ray diffraction analysis reveals some remarkable features of the molecular structures of isomers **1** and **2**. Although the preferred molecular conformation in a solid phase can differ from the one that can be in a solution, the obtained structural information can be useful for interpretation of the kinetic behavior of two structural isomeric derivatives of *ortho*-substituted benzenesulfonyl chloride in the hydrolysis.

Three-dimensional structures of **1** and **2** are presented in Fig. 1; selected crystallographic parameters for two isomers are summarized in Table 2. Noticeable differences in bond lengths and bond angles are observed in the C−SO_2−N fragments of isomeric molecules **1** and **2**. So, in **2**, in contrast to **1**, the C11−S1−N1 bond angle extremely differs from the ideal tetrahedral value of 109.28°; one of two S−O bonds in **2** is significantly lengthened (S1−O1 distances in **1** and 2 are 1.431(1) and 1.529(1) Å, respectively). This fact can be explained by the participation of the O1 atom of both isomeric molecules in the intramolecular hydrogen bridges but with different H-bond strength (Table 3). It also influences onto the conformational parameters of the isomers (torsion angles of C11−S1−N1−C25 and C11−S1−N1−C01 in **1** or **2** are 92.2(1) and −60.6(1)° or 106.6(1) and −81.3(1)°, respectively). There is a need to emphasize once again that the greater lengthening of S1−O1 bond in **2** compared to **1** is apparently caused by the formation of the intramolecular hydrogen bonds that have different strength. Apparently the relevant redistribution of electron density between two S−O bonds within the sulfonate groups of the sulfonyl-amidic fragments, whose the O atoms participate in hydrogen bonding of (S)O···H type, takes place [32,33].

On the other hand, the (C)H···O(S) hydrogen bonds with participating the −SO_2Cl groups also arise in the structures of both isomers. However, these hydrogen bonds in **2** are stronger than in **1** (the O3···H(Me) and O4···H(Ar) distances in **1** are 2.56(2) and 2.41(2) Å, in **2** are 2.27(3) and 2.36(2) Å, respectively). It is particularly remarkable that the shortening of (C)H···O(SOCl) hydrogen bridges correlates with the weakening of S2−Cl1 bond instead of S2−O bonds which are involved into H-bonding (Table 2). It is not difficult to see that the above-said structural parameters of isomeric forms can exercise influence onto reactivity of the appropriate molecules. For instance, the neutral hydrolysis of isomer **2** occurs more readily than **1**.

The presence in the molecules of both isomers of the −SO_2− and −SO_2Cl polar groups provides the formation of intermolecular (S)O···H hydrogen bonds having length 2.37(2)–2.76(2) Å. Owing to cross-linking, the molecules **1** and **2** self-assemble, forming framework of the crystal structures (see Fig. 2). It should be emphasized that the Cl1 atom in **2** is also involved into the formation of (S)Cl···H intermolecular hydrogen bridge (Table 3, Fig. 2) resulting in the weakening of S−Cl bond.

3.2. Stereo-chemical aspect of the neutral hydrolysis process

The crystal chemical analysis of **1** and **2** has revealed that crystal packing of both isomers is provided by non-valent cross-linking (S−O···H hydrogen bridges) of the appropriate molecules with each other. It specifies the mutual orientation of the separate fragments in the appropriate molecules. As can be seen from Fig. 1 and Table 3, the certain orientation of the separate fragments of the bulky molecules also results in formation of intramolecular hydrogen bonds. These intramolecular hydrogen bonds in **2** more strongly fasten the −SO_2Cl group and, thus, prevent its free rotation around the S2−C21 bond. Therefore the molecule **2** is more rigid than of **1**. It facilitates a frontal nucleophilic attack and generates a non-classical transition state of S_N2 type. That is why the molecules of isomer **2** react more readily with water than isomer **1**. The stepwise conversion of isomer **2** during the neutral hydrolysis as well as the

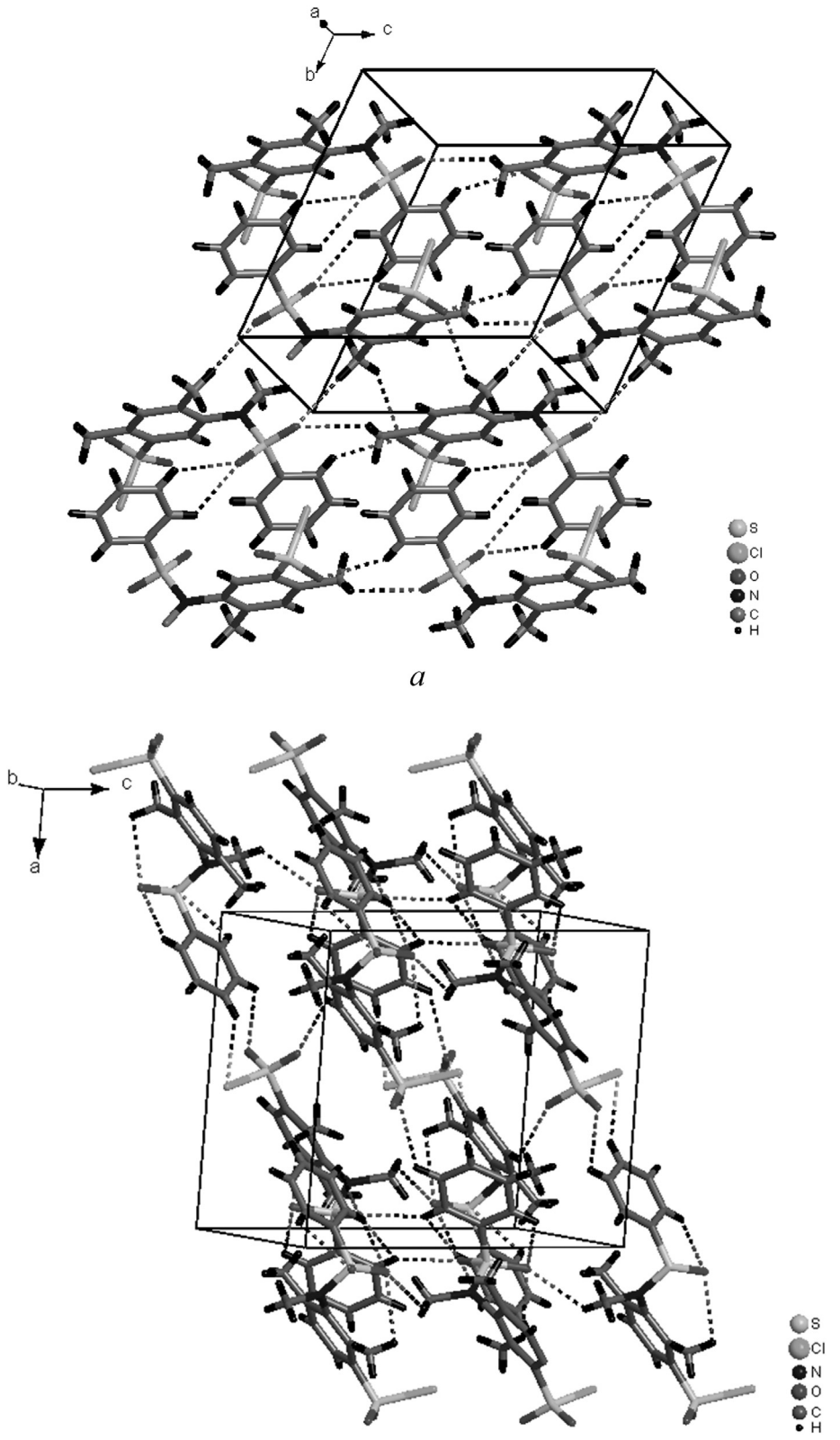

Fig. 2. Crystal packing of the molecules **1** (*a*) and **2** (*b*). Hydrogen bonds are depicted by dot lines.

Table 2
Selected bond lengths (Å) and bond angles (°) in **1** and **2.**

Bonds	1	2	Angles	1	2
S1–O1	1.431(1)	1.529(1)	O1–S1–O2	120.19(7)	121.05(7)
S1–O2	1.435(1)	1.445(1)	O1–S1–N1	106.03(7)	110.92(7)
S1–N1	1.638(1)	1.603(1)	O2–S1–N1	107.46(7)	105.73(7)
S1–C11	1.766(2)	1.685(2)	O1–S1–C11	108.25(7)	109.31(8)
S2–O4	1.422(1)	1.409(1)	O2–S1–C11	107.00(8)	106.02(8)
S2–O3	1.423(1)	1.420(1)	N1–S1–C11	107.30(7)	102.09(8)
S2–C21	1.759(2)	1.712(2)	O4–S2–O3	119.56(8)	122.93(8)
S2–Cl1	2.0392(6)	2.1468(6)	O4–S2–C21	109.49(8)	108.54(8)
			O3–S2–C21	111.71(7)	106.70(8)
			O4–S2–Cl1	105.87(7)	102.37(6)
			O3–S2–Cl1	105.56(6)	107.53(6)
			C21–S2–Cl1	103.09(6)	108.03(6)

stereochemistry of the transition state is represented in Scheme 3 [34].

It should be interesting to consider the influence of strength of the intramolecular hydrogen bonds onto the reactivity of two structural isomers **1** and **2**. So, the quantum-chemical calculations performed for both isomers have revealed that the value of a charge density (δ) on oxygen atoms of the sulfonylchloride group depends on rigidity of the $-SO_2Cl$ group fastening by intramolecular hydrogen bonds (Table 3). As can be seen from Fig. 3, in **2** the δ values on the oxygen atoms participating in formation of the more strong H-bonds (distances O3···H033 and O4···H221 are 2.27(3) and 2.36(2) Å, respectively) are equal −0,514 (on the O3) and −0.518 (on the O4) $\bar{e}$. On the other hand, in **1** the δ values on the same O atoms involved into formation of the less strong H-bonds (distances O3···H032 and O4···H261 are 2.56(2) and 2.41(2) Å, respectively) increase to −0,529 (on the O3) and −0.524 (on the O4) $\bar{e}$.

Such redistribution of electronic density among atoms of the isomers entails specific changes of the geometrical parameters in the molecules **1** and **2.** So, the S2–Cl1 bond in **2** compared to **1** is weaker (Table 2). In **2** the S2–C21 bond length (1.712(2) Å) is shorter than in **1**. The bonds lengths of S2–O3 (1.420(1) Å) and S2–O4 (1.409(1) Å) in **2** somewhat differ between themselves. In **2** the bond angles of C21–S2–O3 and O4–S2–Cl1 are lesser and C21–S2–Cl1 bond angle is larger than those in **1**. Within a distorted $-SO_2Cl$ group of molecule **2** (O3–S2–O4 bond angle is 122.93(8)° instead of 109.28°), a further lengthening of the S2–Cl1 bond is followed by decrease of the absolute value of activation entropy, $|\Delta S^{\neq}|$. It facilitates frontal nucleophilic attack and makes the hydrolysis process by more favorable.

Thus, a shortening of the intramolecular (S)O···H bonds, parameters of which in many respects are specified by stereochemistry of the isomers, causes a certain deficiency of electron density on donor atoms of oxygen. It can be explained by "partial overlap" of atomic orbital, occupied by lone electron pair, of the more electronegative atom (oxygen) with unoccupied atomic orbital of the more electropositive atom (hydrogen). The structural parameters of the intramolecular (S)O···H bonds in **1** and **2** are in good agreement with the calculated energies of the frontier MOs (Fig. 4). In particular, the HOMO level in **2** (−8.368 eV) is more stabilized compared to that in **1** (−8.089 eV).

On the other hand, the H···H contacts springing up between methyl groups and phenyl moieties are also very important for the additional stabilization of molecular conformations upon crystallizing of isomers [35,36]. So, in **1** (Fig. 3a) the H022···H231 and H033···H231 distances are 2.39(4) and 2.25(5) Å, respectively, while in **2** (Fig. 3b) the similar H022···H231 contact is 2.32(3) Å. Nevertheless these intramolecular contacts in both isomers are more lengthened than averaged values of analogous H···H distances (~2.12–2.15 Å) used in R. Bader's theory "Atoms in Molecules" [37] as criterion of influence on conformations stabilization.

Thus, the correlation between charge density values (obtained from quantum-chemical calculations) and length of H···O distances of the intramolecular hydrogen bond (obtained from X-ray crystal structures analyses) is the most objective evaluation parameter. The values of $d_{H\cdots O}$ and δ have an inversely proportional dependence: a shortening of $d_{H\cdots O}$ is accompanied by an increase in δ (Fig. 5).

The reactivity differences observed between two structural isomers, **1** and **2**, in aqueous solution cannot be explained only from the activation enthalpy values, though the increase in reactivity of **2**, as opposed to **1**, is accompanied by the increase in $\Delta H^{\neq}$ value (Table 4). However, such behavior is an untypical for the majority of organic reactions [18,19]. In contrast to it, the absolute value of

Table 3
Hydrogen bonds parameters (Å and °) in **1** and **2.**

H-bonds[a]	D–H	H···A	D···A	D–H···A
1				
C01–H011···O2	1.02(7)	2.53(2)	3.008(9)	106(3)
C12–H121···O2	0.91(5)	2.55(2)	2.903(3)	104(3)
C03–H032···O2^{i}	0.93(3)	2.76(2)	3.388(3)	125(1)
C02–H021···O1	1.00(3)	2.64(2)	3.191(7)	116(3)
C23–H231···O4^{ii}	0.97(3)	2.34(2)	3.338(3)	171(3)
C26–H261···O4	0.97(3)	2.41(2)	2.843(4)	106(2)
C03–H032···O3	0.93(3)	2.56(2)	3.091(4)	116(4)
C12–H121···O3^{iii}	0.91(5)	2.67(2)	3.403(4)	141(4)
2				
C03–H032···O1	0.98(2)	2.68(2)	3.076(2)	104(2)
C16–H161···O1	0.94(2)	2.50(2)	2.826(3)	100(2)
C01–H011···O1^{iv}	0.93(2)	2.63(2)	3.246(3)	124(2)
C16–H161···O2^{v}	0.94(2)	2.48(2)	3.126(2)	126(2)
C12–H121···O2	0.94(2)	2.63(2)	2.878(3)	96(2)
C12–H121···O2^{vi}	0.94(2)	2.51(2)	3.359(2)	151(2)
C03–H033···O3	0.85(4)	2.27(3)	2.895(2)	131(3)
C23–H231···O3^{vii}	0.95(2)	2.75(2)	3.300(2)	117(2)
C22–H221···O4	0.92(2)	2.36(2)	2.750(2)	106(2)
C13–H131···O4^{viii}	0.98(2)	2.75(2)	3.395(3)	124(2)
C14–H141···Cl1^{viii}	0.87(2)	2.83(2)	3.460(2)	130(2)

[a] Symmetry codes: (i) $x, y, -1+z$; (ii) $1+x, y, z$; (iii) $x, y, 1+z$; (iv) $x, 0.5-y, 0.5+z$; (v) $-x, 0.5+y, 0.5-z$; (vi) $-x, -y, -z$; (vii) $1-x, 0.5+y, 0.5-z$; (viii) $-1+x, 0.5-y, 0.5+z$.

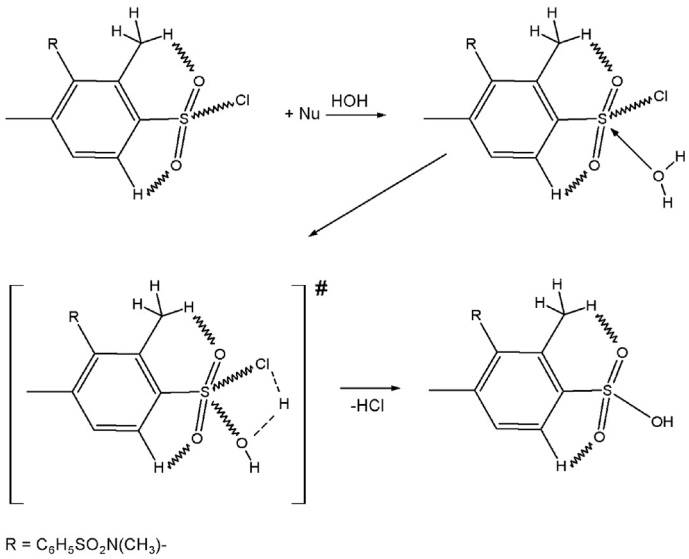

R = $C_6H_5SO_2N(CH_3)$-

Scheme 3. Stereochemistry of the neutral hydrolysis reaction of the 2,4-dimethyl-3-[methyl(phenylsulfonyl)amino]benzenesulfonyl chloride (**2**).

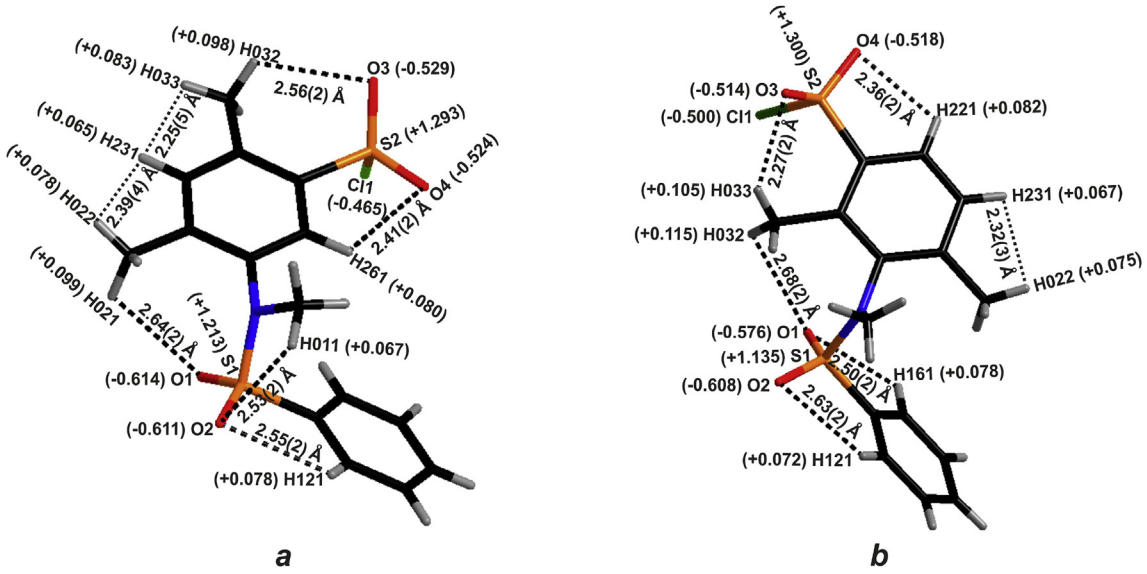

Fig. 3. Charge density (±δ, $\bar{e}$) distribution on the atoms of the $-SO_2Cl$ and $-SO_2-$ groups in the molecule **1** (*a*) and **2** (*b*).

activation entropy, $|\Delta S^{\neq}|$, is lower for **2** than for **1**. Thus, there are losses of activation enthalpy for **2** in comparison with **1**, since after formation of the activated complex, steric parameters of the transition state any more cannot be a rate-determining factor of the hydrolysis reaction. Greater rate of the neutral hydrolysis observed for **2** can be explained by the elimination of steric hindrances for the potential nucleophilic attack in the initial state of **2** and by the formation of the less ordered transition state [38].

Thus, the study of the crystal and electronic structure of two molecular isomers **1** and **2** has provided by reliable information on the stereochemistry of the initial and transitional states of these molecules in aqueous solution. For the reasons given above, these two structural isomers show the different reactivity in the hydrolysis process.

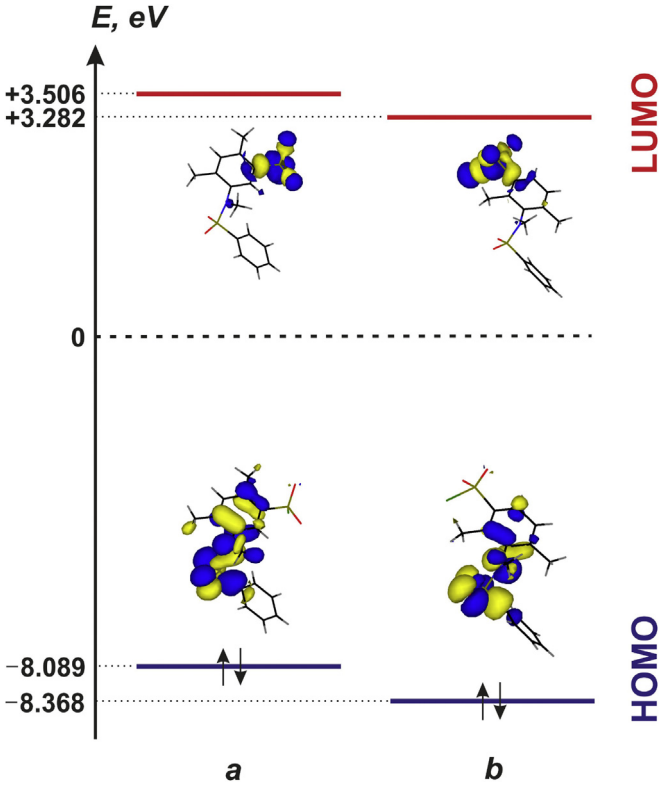

Fig. 4. Calculated frontier MO energies of **1** (*a*) and **2** (*b*).

4. Conclusions

Thus, two new structural isomers of *ortho*-alkyl derivatives of benzenesulfonyl chloride have been synthesized. Both obtained isomeric forms – 2,4-dimethyl-5-[methyl(phenylsulfonyl)amino]-

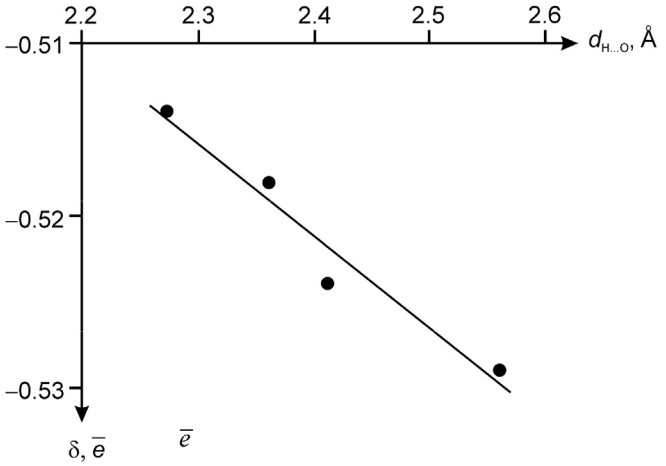

Fig. 5. Plot of $d_{H\cdots O}$ versus δ for both isomeric forms ($r = 0.97$).

Table 4
The effective rate constants and thermodynamic data for reactions of the neutral hydrolysis of **1** and **2.**

Isomer	k_{eff} 10^4, s^{-1}			$\Delta H^{\neq}$, kJ mol^{-1}	$-\Delta S^{\neq}$, J mol^{-1} K^{-1}	$\Delta G^{\neq}_{313}$, kJ mol^{-1}
	303 K	313 K	323 K			
1	0.603	1.16	2.17	49.5 ± 0.5	186 ± 2	108 ± 1
2	0.686	1.49	3.79	66.8 ± 4.9	131 ± 15	108 ± 8

benzenesulfonyl chloride (**1**) and 2,4-dimethyl-3-[methyl(phenylsulfonyl)amino]-benzenesulfonyl chloride (**2**) – are organized as molecular crystals. The crystal chemical analysis of isomers **1** and **2** has revealed that polar groups (−SO_2Cl and −SO_2−) in the sterically hindered molecules generate the intramolecular hydrogen bonds of a (C)H···O(S) type. Both structures are stabilized by the branched system of intermolecular hydrogen bridges of the (C)H···O and (C)H···Cl types.

The crystal structure data and quantum-chemical calculations have been used for interpretation of behavior of the bulky molecules **1** and **2** in aqueous solution. Unlike **1**, the molecule **2** has a more rigid structure and a more "labile" S–Cl bond. It creates favorable conditions for reaction of nucleophilic substitution on substrate in **2** and stabilizes a bimolecular transition state. The particular molecular structure promotes the certain reallocation of charge density on atoms in molecule **2** and leads to a possible frontal attack of nucleophilic agent and formation of non-classical transition state of S_N2 type. It is reverberated on values of thermodynamic parameters of the transition state and the hyperreactivity of the isomer **2**.

Appendix A. Supplementary data

Supplementary data related to this article can be found at http://dx.doi.org/10.1016/j.molstruc.2017.02.016/

References

[1] H. Cerfontain, Mechanistic Aspects in Aromatic Sulfonation and Desulfonation, Interscience Publishers, New York, London, Sydney, Toronto, 1968.
[2] A. Kalir, H. Kalir, in: The Chemistry of Sulphonic Acids, Esters and Their Derivatives, Saul Patai, Zvi Rappoport, John Wiley & Sons, Ltd., Chichester, New York, Brisbane, Toronto, Singapore, 1991, pp. 767–787.
[3] E. G. Everett, A. O. Julian, A. P. Silvio, Substituted-urea sulfonic acid herbicides, US Patent No 2801911 A, 1957.
[4] I. Daisuke, U. Hiroaki, A. Emi, K. Tomoyuki, Aromatic sulfonic acid derivative, sulfonic acid group-containing polymer, block co-polymer, polymer electrolyte material, polymer electrolyte molded body, and solid polymer fuel cell. US Patent No 0213671 A1, 2014.
[5] R. R. Grinstead, Metallurgical extractant system. US Patent No 4382872 A, 1983.
[6] F. M Higgins, W. M. Murch, Dye powder compositions. US Patent No 2058489 A, 1936.
[7] R. L. Brandt, Preparation of aliphatic-aromatic sulphonates. US Patent No 2244512 A, 1939.
[8] A. Ogino, Y. Midorikawa, Y. Sato, K. Inada, M. Higuchi, M. Suga, Phenolsulfonic acid aryl ester, developing agent, and heat-sensitive recording material. EU Patent No 2774916 A1, 2014.
[9] J.L. Kice, Adv. Phys. Org. Chem. 17 (1980) 65.
[10] Z.H. Ryu, S.W. Lee, M.J. D'Souza, L. Yaakoubd, S.E. Feld, D.N. Kevill, Int. J. Mol. Sci. 9 (2008) 2639.
[11] M.J. D'Souza, L. Yaakoubd, S.L. Mlynarski, D.N. Kevill, Int. J. Mol. Sci. 9 (2008) 914.
[12] T.W. Bentley, J. Org. Chem. 73 (2008) 6251.
[13] T.W. Bentley, R.O. Jones, Dae Ho Kang, In Sun Koo, J. Phys. Org. Chem. 22 (2009) 799.
[14] M. Jaiswal, P.V. Khadikar, A. Scozzafavo, C.T. Supuran, Bioorg. Med. Chem. Lett. 14 (2004) 3283.
[15] V.K. Agrawal, S. Shriwastava, P.V. Khadikar, C.T. Supuran, Bioorg. Med. Chem. 11 (2003) 5353.
[16] Ph. D. Stein, D.M. Floyd, S. Bisaha, J. Dickey, R.N. Girotra, J.Z. Gougoutas, M. Kozlowski, L.V.G. Lee, E.C.-K. Liu, M.F. Malley, D. McMullen, C. Mitchell, S. Moreland, N. Murugesan, R. Serafino, M.L. Webb, R. Zhang, J.T. Hunt, J. Med. Chem. 38 (1995) 1344.
[17] T.W. Bell, S. Anugu, P. Bailey, V.J. Catalano, K. Dey, M.G.B. Drew, N.H. Duffy, Q. Jin, M.F. Samala, A. Sodoma, W.H. Welch, J. Med. Chem. 49 (2006) 1291.
[18] R. Schmid, V.N. Sapunov, Non-formal Kinetics: in Search for Chemical for Chemical Reaction Pathways, Verlag Chemie, Weinheim, 1982.
[19] M.B. Smith, J. March, March's Advanced Organic Chemistry. Reactions, Mechanisms, and Structure, John Wiley & Sons, Inc., Hoboken, 2007.
[20] M. Iazykov, M.L. Canle, J.A. Santaballa, L. Rublova, Int. J. Chem. Kinet. 47 (2015) 744.
[21] I.S. Koo, T.W. Bentley, D.H. Kang, J. Chem. Soc. Perkin Trans. 2 (1991) 175.
[22] M. Mikozajczyk, M. Gajl, W. Reimschtisel, Tetrahedron Lett. 16 (1975) 1325.
[23] A.R. Haughton, R.M. Laird, M.J. Spencc, J. Chem. Soc. Perkin Trans. 2 (1975) 637.
[24] M. Iazykov, L. Rublova, L.M. Canle, J.A. Santaballa, J. Phys. Org. Chem. 30 (2017) e3588.
[25] I.S. Koo, T.W. Bentley, D.H. Kang, I. Lee, J. Chem. Soc. Perkin Trans. 2 (1991) 175.
[26] F.P. Ballistreri, A. Cantone, E. Maccarone, G.A. Tomaselli, M. Tripolone, J. Chem. Soc. Perkin Trans. 2 (1981) 438.
[27] Oxford Diffraction, CrysAlis CCD, Data Collection GUI for CCD and CrysAlis RED, CCD Data Reduction GUI, Version 1.171, Oxford Diffraction, Wroclaw, Poland, 2002.
[28] G.M. Sheldrick, Acta Crystallogr. A64 (2008) 112.
[29] K. Brandenburg, Diamond, Version 2.1c, Crystal Impact GbR, Bonn, 1998.
[30] R. Schmid, V.N. Sapunov, Non-formal Kinetics: in Search for Chemical Reaction Pathways, Verlag Chemie, Weinheim, 1982.
[31] HyperChem, Molecular Modeling System, Hypercube, Inc., Florida, 2010. Release 8.0.6.
[32] G.R. Desiraju, Dalton Trans. 21 (2000) 3745.
[33] G.R. Desiraju, Acc. Chem. Res. 35 (2002) 565.
[34] S. Okovytyy, L. Rublova, V. Levandovsky, J. Leszczynski, in: Abstr. of Papers, 11th Souther School on Computational Chemistry and Materials Science, Mississippi, 2011, p. 42.
[35] G.V. Baryshnikov, B.F. Minaev, V.A. Minaeva, A.T. Baryshnikova, M. Pittelkow, J. Mol. Struct. 1026 (2012) 127.
[36] I.S. Bushmarinov, K.A. Lyssenko, M. Yu. Antipin, Rus. Chem. Rev. 78 (2009) 283.
[37] G.V. Baryshnikov, B.F. Minaev, V.A. Minaeva, J. Struct. Chem. 52 (2011) 1051.
[38] L.I. Rublova, V.Y. Levandovsky, N.A. Yazikov, T.S. Popovich, in: Abstr. of Papers, XVIII International Conference on Chemical Thermodynamics, Samara, vol. 2, 2011, p. 77.